Plant Science 251 (2016) 128–138

Contents lists available at ScienceDirect

Plant Science

journal homepage: www.elsevier.com/locate/plantsci

Effects of abiotic stress on physiological plasticity and water use of *Setaria viridis* (L.)☆

Prasenjit Saha[2], Nir Sade[2], Ahmad Arzani[1], Maria del Mar Rubio Wilhelmi, Kevin M. Coe, Bosheng Li, Eduardo Blumwald*

Department of Plant Sciences, University of California Davis, Davis, CA 95616, USA

ARTICLE INFO

Article history:
Received 20 February 2016
Received in revised form 3 June 2016
Accepted 16 June 2016
Available online 20 July 2016

Keywords:
Accessions
Physiological plasticity
Setaria viridis
Water-deficit stress
Heat stress
Stress responses

ABSTRACT

The emerging model *Setaria viridis* with its C4 photosynthesis and adaptation to hot and dry locations is a promising system to investigate water use and abiotic stress tolerance. We investigated the physiological plasticity of six *S. viridis* natural accessions that originated from different regions of the world under normal conditions and conditions of water-deficit stress and high temperatures. Accessions Zha-1, A10.1 and Ula-1 showed significantly higher leaf water potential (Ψ_{leaf}), photosynthesis (A), transpiration (E), and stomatal conductance (g_s) rates compared to Ast-1, Aba-1 and Sha-1 when grown under stress conditions. Expression analysis of genes associated with C4 photosynthesis, aquaporins, ABA biosynthesis and signaling including genes involved in stress revealed an increased sensitivity of Ast-1, Aba-1 and Sha-1 to stresses. Correlation analysis of gene expression data with physiological and biochemical changes characterized A10.1 and Ast-1 as two extreme tolerant and sensitive accessions originated from United States and Azerbaijan under water-deficit and heat stress, respectively. Although preliminary, our study demonstrated the plasticity of *S. viridis* accessions under stress, and allows the identification of tolerant and sensitive accessions that could be use to study the mechanisms associated with stress tolerance and to characterize of the regulatory networks involved in C4 grasses.

1. Introduction

Monocot C4 cereal grains and grasses belonging to the Panicoideae subfamily comprise crops that are major sources of food and feedstock, such as maize (*Zea mays*), sorghum (*Sorghum bicolor*), sugarcane (*Saccharum officinarum*), pearl millet (*Pennisetum glaucum*), switchgrass (*Panicum virgatum*), etc. Because most C4 plants are well adapted to high light intensities, elevated temperatures and relatively poor soils, they have attracted significant interest and are becoming the focus of intense research [1,2]. Although, considerable advancement towards the understanding of the molecular and biochemical pathways associated with C4 metabolism [3–5] and the relative tolerance of C4 crops to abiotic stress has been made [6–8], the progress of these researches has been hampered because of their big size, large and/or polyploid genome and long generation times. *Setaria viridis* has a C4 metabolism, small genome (approximately 510 Mb), short life cycle and simple growth requirements [3]. Moreover, the recent demonstration of a fast and simple spike-dip-mediated genetic transformation [9] makes *S. viridis* an ideal model plant for the study of abiotic stress in Panicoideae crops.

Wild relatives of cultivated crops perform better under adverse environmental conditions, and often deliver a valuable gene pool for abiotic stress tolerance [10]. In addition, natural populations of crop species inhabiting wide locations showed phenotypic plasticity to stress based on their genetic background [11]. Recently, phenotypic variability [12,13], as well as molecular genetic mapping and sequencing [14–16] of natural populations of *S. viridis*, a wild ancestor of cultivated foxtail millet (*S. italica*), have been reported. Although, progress has been made in the genome sequencing [17], including understanding the regulation of gene expression related to the C4 pathway [4], characterization of its germplasm to abiotic stress is lacking. Thus, understanding the phenotypic plasticity of its natural accessions to abiotic stress is crucial to reveal the molecular mechanism of stress tolerance and water use efficiency (WUE).

Here we investigated six *S. viridis* natural accessions originated from different areas of the world under water-deficits, high

☆ This article is part of a special issue entitled "Water-use Efficiency in plants", published in Plant Science 251, 2016.

* Corresponding author.
E-mail address: eblumwald@ucdavis.edu (E. Blumwald).
[1] Current address: Department of Agronomy and Plant Breeding, College of Agriculture, Isfahan University of Technology, Isfahan 84156, Iran.
[2] Authors contributed equally to this work.

http://dx.doi.org/10.1016/j.plantsci.2016.06.011
0168-9452/

temperature and a combination of both stress conditions. We demonstrated the plasticity of accessions in the reduction of leaf water potential, photosynthetic rates and stomatal closure at the physiological level. We also showed that stress related gene expression changes at the molecular level and biochemical changes such as scavenging of reactive oxygen species (ROS), accumulation of osmolytes and reallocation of metabolites were different among accessions under stress. This preliminary study allowed us to distinguish between tolerant and sensitive accessions as a function of the water usage and their responses to abiotic stress.

2. Materials and methods

2.1. Plant materials and growth habitat

Seeds of six *Setaria viridis* (L.) Thell. (Zha-1, A10.1, Ula-1, Ast-1, Aba-1 and Sha-1) accessions were obtained from the Germplasm Resources Information Network (GRIN, http://www.ars-grin.gov/), United States Department of Agriculture (USDA) and germinated in trays (27.9 cm × 54.3 cm) (McConkey, Sumner, WA) containing moist agronomy mix (equal parts of redwood compost, sand and peat moss) in the greenhouse conditions at 28 ± 2 °C with 50% relative humidity under a 16 h day/8 h night photoperiod and 550 μ mol m^{-2} sec^{-1} light intensity. The characteristic, origin and distribution of these six accessions are given in Table 1. At 10 days post germination (DPG), seedlings were transferred to plastic pots (10.2 cm × 8.2 cm) (McConkey) containing equal amount of agronomy mix soil and grown in the same greenhouse conditions.

2.2. Abiotic stress treatments

Before the application of water-deficit stress and heat treatments to the *S. viridis* accessions, 10 DPG seedlings of an average height of 6.9 ± 0.8 cm were grown in pots in the greenhouse under the conditions described above for 10 days. Plants were watered to field capacity every alternate day with deionized water and fertilized (once a week) with a solution of 100 g N:P:K (20:10:20) and 100 g ammonium sulphate in 20 L of deionized water. During this period with the progression of stress treatments Zha-1, A10.1, Ula-1 and Ast-1 initiated flowering while Aba-1 and Sha-1 did not flower until the end of stress treatments.

For water-deficit treatments, water stress (WS) was applied by withholding the water supply to pots containing 20 DPG plants for 7–10 days in the same greenhouse conditions. After this initial period of water withholding, the soil water content (SWC) of each pot was measured using a ProCheck soil moisture meter (Decagon Devices, Inc. Pullman, WA, USA) until the SWC reached to 30% and when more than 50% of the seedling populations of the different accessions showed visible stress phenotypes (initiation of leaf rolling and dropping or wilting), the SWC was maintained at 30% for an additional 5–8 days.

For heat stress (HS), 20 DPG plants were placed in a controlled environmental chamber (Conviron, Pembina, ND, USA) under a 16 h daytime (light intensity of 550 μ $molm^{-2}$ sec^{-1}) and the temperature raised from 28 °C to 42 °C, the seedlings were exposed to 42 °C for 2 h, and the temperature was brought back to 28 °C afterwards, followed by 8 h dark at 25 °C. Relative humidity was kept at 50%. These temperature treatments were repeated daily for 15 days for all accessions.

For water-deficit and heat stress combination treatments (WSH), a set of plants (n = 6) was treated as described for HS treatments while the plants were kept at a SWC as described for WS (see above).

A well-watered (WW) set of plants with 100% SWC from all accessions were grown under the same greenhouse conditions with similar irrigation and fertilization regimes as described before. Each experimental setup included randomized WW, WS, HS and WSH sets of plants in four biological replicates for each of the six *S. viridis* accessions. Three separate experiments were conducted during August–September 2014, November–December 2014 and March–April 2015. After 15 days of treatments and at the end of each experiment (when plants were 35 days-old), physiological measurements were conducted on three biological replicates while leaves of one replicate were harvested followed by quick freezing in liquid nitrogen at the same daytime period (10 a.m. to 12 noon). All samples were homogenized to fine powder in liquid nitrogen and stored at −80 °C until further use.

2.3. Physiological measurements

Leaf water potential (Ψ_{leaf}) was measured from an excised flag leaf or top leaf whichever was available from 10 days post treatment (DPT) plants under WS and HS, as well as WW, when plants were 30 days-old from each accession using a pressure chamber instrument (Model 600, PMS Instrument Company, Albany, OR, USA) attached to a portable nitrogen (N_2) tank. An apical portion of a leaf was excised with a sharp razor blade and immediately inserted inside the stainless steel chamber, and closed tightly. The N_2 gas was slowly released to gradually increase the inside pressure of the chamber and the oozing out of sap was monitored using a lighted hand lens. The value of the pressure gauge was recorded when first emergence of leaf sap was monitored. All measurements were taken between 10 a.m. to12 noon.

Gas exchange measurements were carried out using a Li-Cor 6400 open gas exchange system (Li-Cor, Lincoln, NE, USA) calibrated at 1800 μ $molm^{-2}$ s^{-1} saturating light condition and 400 ppm ambient CO_2 with a 50–60% relative humidity and 28 °C as described before. Each measurement was recorded at steady state on 15 DPT plant from each of the treatments mentioned above.

Leaf area measurements were taken at the end of each experiment when plants were 35 days-old using a LI-3100 Area Meter (Li-Cor). For biomass dry weight (DW), above ground plant parts

Table 1
Distribution and associated parameters of *Setaria viridis* accessions used in this study.

Parameters*	Accessions					
Code	Zha-1	A10.1	Ula-1	Ast-1	Aba-1	Sha-1
Accession	Ames 28193	PI 669942/Ames 31045	PI 649320	PI 223677	PI 230135	PI 408811
Plant name	132	A10.1	98HT-80	Dekker 1851	Dekker 1850	UI 4833
Origin (country)	Kazakhstan	United States	Mongolia	Azerbaijan	Iran	China
Area	Zhangiztobe	NA	Ulaanbaatar	Astara	Abali	Shaanxi
Latitude	49.1286	NA	48.1339	38.4561	35.7624	34.2500
Longitude	81.1078	NA	110.2281	48.8786	51.9653	108.8667
Elevation (meter)	517.9	NA	1026.9	274.3	1828.8	405.1

* Data obtained from GRIN, USDA website. NA, not available.

was cut at soil level and dried in an oven at 80 °C for 5 days before weighing. DW penalty was calculated as relative ratio of DW under WS and HS with respective to WW (DW_{WSorHS}/DW_{WW}).

2.4. Molecular analyses

Selection of candidate reference and target genes was performed as described before in Ref. [18]. The list of genes tested for the identification of suitable reference gene(s) for gene expression data normalization using qRT-PCR is given in Supplementary Table S1 in the online version at DOI: 10.1016/j.plantsci.2016.06.011. Selection of best reference gene(s) was conducted following the procedure described earlier [18,19] using the computer-based RefFinder [20] (see Supplementary Table S2 in the online version at DOI: 10.1016/j.plantsci.2016.06.011). Primers were designed using Primer3Plus software (http://www.bioinformatics.nl/cgi-bin/primer3plus/primer3plus.cgi) considering the parameters specific for qRT-PCR [21]. The sequences with detailed parameters of primer pairs of candidate reference and target genes are given in Supplementary Table S1 in the online version at DOI: 10.1016/j.plantsci.2016.06.011, respectively.

For gene expression analyses, RNA was extracted from 100 mg of frozen ground leaf tissue of WS, HS, and WW samples as described before [22], and first-strand complementary DNA (cDNA) synthesis, followed by qRT-PCR were performed as described before [18]. Analysis of relative gene expression was performed after normalization with two best reference genes according to Ref. [23].

2.5. Biochemical quantifications

Extraction and quantification of abscisic acid (ABA) were conducted as described earlier by Ref. [24] using 50 mg of frozen ground leaf in 100% (v/v) methanol containing 0.5 g/L citric acid monohydrate and 100 mg/L butylated hydroxytoluene (BHT). ABA contents were determined using enzyme-linked immunosorbent assay (ELISA) as described before [25] following manufacture instruction.

A total of 100 mg of frozen ground tissue was homogenized in a 2 ml SealRite microcentrifuge tube containing 1 ml of extraction buffer (50 mM Tris–HCl, pH 7.5; 5% w/v sucrose; 5% w/v PVP; 50 mM ascorbic acid) using 3.2 mm stainless steel beads in an automated shaker SO–10 M (Fluid Management, Wheeling, IL, USA). The homogenate was centrifuged and the supernatant was used as a source for total protein and enzyme assay as described elsewhere [26].

The Bradford assay [27] method was used for total protein quantification using bovine serum albumin (BSA) as a standard. Catalase activity was assessed as the decomposition of H_2O_2 by measuring the decrease of absorbance at 240 nm [28]. Chlorophyll content was measured from 100 mg of frozen ground tissue homogenized in 1 ml of *N*,*N*-dimethyl formamide (DMF) in the dark and the absorbance of the supernatant was recorded at 647 nm and 664 nm [29,30]. Malondialdehyde (MDA) content was measured as described before [30]. Proline was extracted from 100 mg of ground plant material by heating plant material for 20 min twice with 80% ethanol and once with 50% ethanol as described by Ref. [31]. SPS activity measurements were conducted based on Ref. [32] using 50 mM Hepes/NaOH, pH 7.5 (Sigma), 15 mM $MgCl_2$ (Sigma), 25 mM Fructose (Sigma), and 25 mM UDP-Glucose. Sugars were quantified using an anthrone assay [33], and absorbance at 650 or 595 nm were measured using sucrose as a standard. Extraction and measurement of the total soluble sugars (SS) from leaf tissue samples were carried out as described by Ref. [30]. All reactions were performed in two technical replicates and all measurements were made in a 96 well BioTek SynergyMx microplate reader (BioTek Instruments, Inc., Winooski, VT).

2.6. Statistical analysis

Physiological measurements were carried out in nine biological replicates whereas molecular analyses and biochemical quantifications were conducted in three biological replicates. Calculations of means from biological replicates with standard errors (SE) including figures were created using Microsoft Excel (version 2010). Tukey-Kramer HSD tests was used to evaluate significant differences at $P \leq 0.05$ level in JMP (version 7.0.2) software (SAS Institute Inc. Cary, NC). The normal distribution of the data and the homogeneity of variances were verified with the Kolmogorov-Smirnov and Bartlett's tests, respectively, before being subjected to analysis of variance (ANOVA). Data were analyzed as a split-plot design, where stress conditions (WW, WS and HS) were used as a fixed-plot factor while accession and stress × accession as random effects in ANOVA using PROC GLM of SAS version 9.3 (SAS Institute, 2011). For correlation analyses, physiological, biochemical and gene expression data from WS and HS were normalized with WW and transformed to Log_{10} values. To visualize the differences among accessions exposed to stress, we performed Pearson Correlation Coefficients (PCC) of Log_{10} transformed values and conducted hierarchical clustering. Heatmaps illustrating positive (yellow) and negative (blue) correlations under WS and HS were generated using R statistical software [34].

3. Results

3.1. Physiological responses to WS and HS

In this study we evaluated six *S. viridis* natural accessions which were originated from wide areas world-wide (Table 1) for their tolerance to WS and HS. These accessions showed differential patterns of physiological responses to WS and HS (Fig. 1). Measurements of leaf water potential (Ψ_{leaf}) after 10 DPT revealed significant changes in leaf water status (Fig. 1a). Under WW conditions, Zha-1, A10.1 and Ula-1 showed relatively lower Ψ_{leaf} (−0.34 to −0.38 MPa) as compared to Ast-1, Aba-1 and Sha-1 (−0.15 to −0.20 MPa). When these accessions were exposed to WS, Ast-1, Aba-1 and Sha-1 displayed a marked decrease in leaf water potential with an average Ψ_{leaf} of −1.1 MPa, whereas Zha-1, A10.1 and Ula-1 maintained a Ψ_{leaf} in the range of −0.40 MPa to −0.52 MPa. In case of HS, all the accessions demonstrated a significant reduction in leaf water potential, with lowest and highest Ψ_{leaf} of −2.13 MPa and −0.71 MPa in Ast-1 and Zha-1, respectively (Fig. 1a).

Gas exchange measurements showed a differential performance of accessions subjected to WW, WS and HS (Fig. 1b–d). Under WW conditions, maximum and minimum rates of photosynthesis (*A*) and transpiration (*E*) were recorded in A10.1 and Sha-1, respectively. The rates of *A* and *E* were significantly higher in Zha-1, A10.1 and Ula-1 as compared to Ast-1, Aba-1 and Sha-1 under both WS and HS treatments. In general *A* and *E* were severely affected by HS in most of the accessions where Ast-1 and Aba-1 showed the strongest reduction of *A* (86.3% and 93.3%, respectively) and *E* (76.3% and 86.1%, respectively) under both WS and HS treatments (Fig. 1b–c). Measurements of stomatal conductance (g_s) suggested that H_2O/CO_2 exchange was relatively less affected by WS and HS in Zha-1, A10.1 and Ula-1 as compared to Ast-1, Aba-1 and Sha-1 (Fig. 1d).

At the end of the experiment all accessions grown under WW showed no significant difference in the total leaf area (Fig. 2a), while above-ground biomass DW of Zha-1 and Ula-1 was significantly lower compared to A10.1, Ast-1, Aba-1 and Sha-1 under similar con-

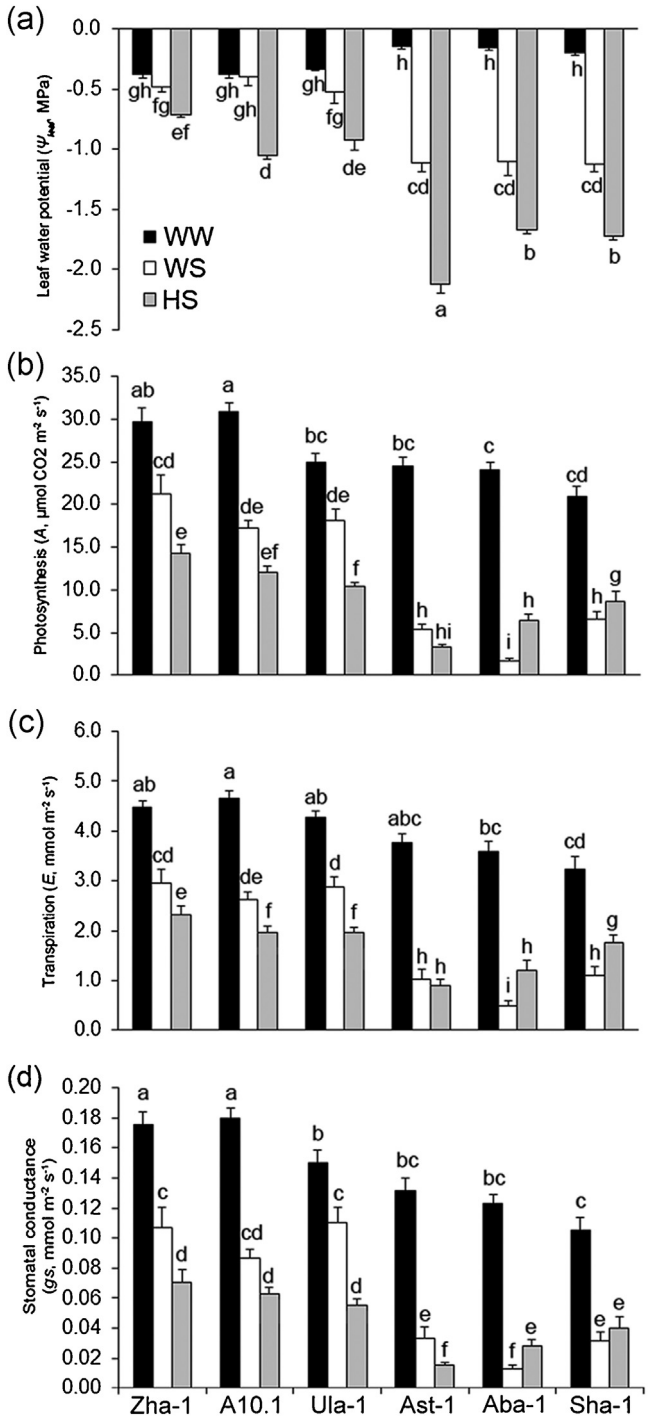

Fig. 1. Physiological responses of *Setaria viridis* accessions to WW, WS and HS conditions. (a) Leaf water potential (Ψ_{leaf}) of accessions measured after 10 DPT using a pressure chamber. Gas exchange measurements of (b) photosynthesis (A) and (c) rates of transpiration (E) and (d) stomatal conductance (g_s) after 15 DPT using a Li-Cor 6400 portable gas exchange system, respectively. Black, white and grey bars represent the Mean ± SE (n = 9) from well-water (WW), water-deficit stress (WS) and heat stress (HS) treated plants and letters on the bars indicate significant differences at $P \leq 0.05$ level as tested by Tukey-Kramer HSD.

ditions (Fig. 2b). WS and WHS showed a stronger effect of biomass DW reduction than HS in Ast-1, Aba-1 and Sha-1 compared to Zha-1, A10.1 and Ula-1 (Fig. 2b) which was clearly documented in biomass DW penalty (see Supplementary Fig. S1 in the online version at DOI: 10.1016/j.plantsci.2016.06.011).

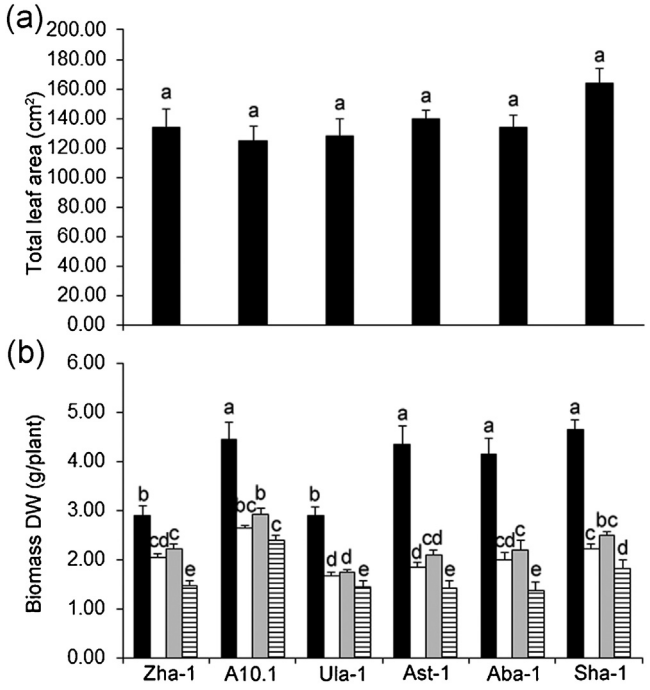

Fig. 2. Leaf area of *Setaria viridis* accessions under well-water (WW) conditions and the effect of water stress (WS), heat stress (HS) and water-heat stress (WHS) on biomass dry weight (DW) after 15 days of stress treatments. Black, white, grey and lined bars represent mean ± SE (n = 6–9) values of WW, WS, HS and WHS combined treatments and letters on the bars indicate significant differences at $P \leq 0.05$ level as tested by Tukey-Kramer HSD.

3.2. Identification and selection of suitable reference genes for gene expression analysis under abiotic stress conditions

Prior to performing gene expression analysis under abiotic stress conditions in the different *S. viridis* accessions, we sought to identify suitable reference gene/s for accurate transcript normalization using qRT-PCR. We searched for candidate reference genes previously tested in Arabidopsis, rice and foxtail millet, and found the orthologous locus identifiers and/or GenBank accession numbers of the potential candidate reference genes from *S. italica*, a cultivated close relative of *S. viridis*, using orthologous group search in Phytozome and/or BLASTN search in the NCBI GenBank. We selected a total of 14 candidate reference genes (see Supplementary Table S1 in the online version at DOI: 10.1016/j.plantsci.2016.06.011) and tested their expression stability in a set of samples which included WW, WS, HS and salt-stressed (SS) plants in six biological with three technical replicates from the A10.1 accession using qRT-PCR. Analysis of melt curves revealed a single dominant peak of the specific amplicon with no detectable amplifications in the no-template controls (NTCs), suggesting the absence of any primer dimers and specific amplification from the respective primer pair (see Supplementary Fig. S2 in the online version at DOI: 10.1016/j.plantsci.2016.06.011). Detailed parameters, including analysis of PCR efficiency (E) using LinRegPCR software [35], correlation coefficients (R^2) of PCR efficiency values and coefficient of variance (CV) of threshold cycle (C_T) values are given in Supplementary Table S1 in the online version at DOI: 10.1016/j.plantsci.2016.06.011. Further analysis of individual C_T values in RefFinder software recommended *tubulin-α* (*TUA*) and *initiation factor 4A* (*IF4A*) with 2.0 and 2.3 of overall comprehensive geomean ranking values, respectively, as the best two reference genes for reliable transcript normalization using qRT-PCR in *S. viridis* (see Supplementary Table S2 in the online version at DOI: 10.1016/j.plantsci.2016.06.011).

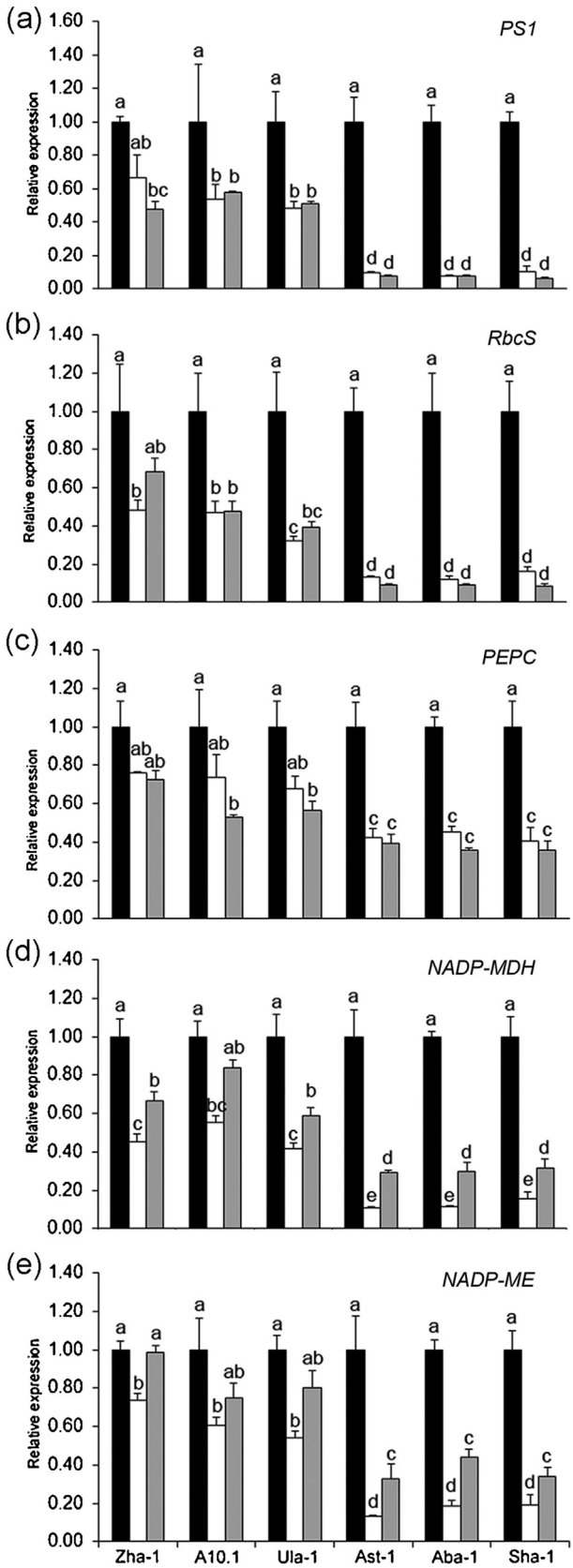

Fig. 3. Effect of WS and HS on photosynthesis, CO_2 exchange and carbon assimilation associated gene expression in *Setaria viridis* accessions. Quantitative measurements of mean relative expression patterns of (a) *PS1*, (b) *RbcS*, (c) *PEPC*, (d) *NADP-MDH* (e) *NADP-ME* genes as determined by qRT-PCR. Black, white and grey bars represent the Mean ± SE (n = 3) of $2^{-\Delta\Delta CT}$ values after normalization with reference genes (*TAU* + *IF4A*) from RNA samples of well-water (WW), water stress (WS) and heat stress (HS) treated plants and letters on the bars indicate significant differences at $P \leq 0.05$ level as tested by Tukey-Kramer HSD. See Table S1 for reference and target genes.

3.3. Monitoring expression pattern of photosynthesis and aquaporin-related genes under WS and HS

We monitored the expression patterns of genes associated with photosynthesis, C4-CO_2 assimilation and aquaporin water channels of the *S. viridis* accessions under WS and HS using qRT-PCR (Figs. 3 and 4). The expression of *photosystem 1* (*PS1*) and *ribulose bisphosphate carboxylase small subunit* (*RbcS*) decreased significantly in all accessions under WS and HS, with Ast-1, Aba-1 and Sha-1 displaying a more pronounced decrease in transcripts abundance (Fig. 3a,b). We also examined the expression of three genes associated with CO_2 assimilation during C4 carbon fixation (Fig. 3c–e). *Phosphoenolpyruvate carboxylase* (*PEPC*) and *NADP-malate dehydrogenase* (*NADP-MDH*), transcripts are rel-

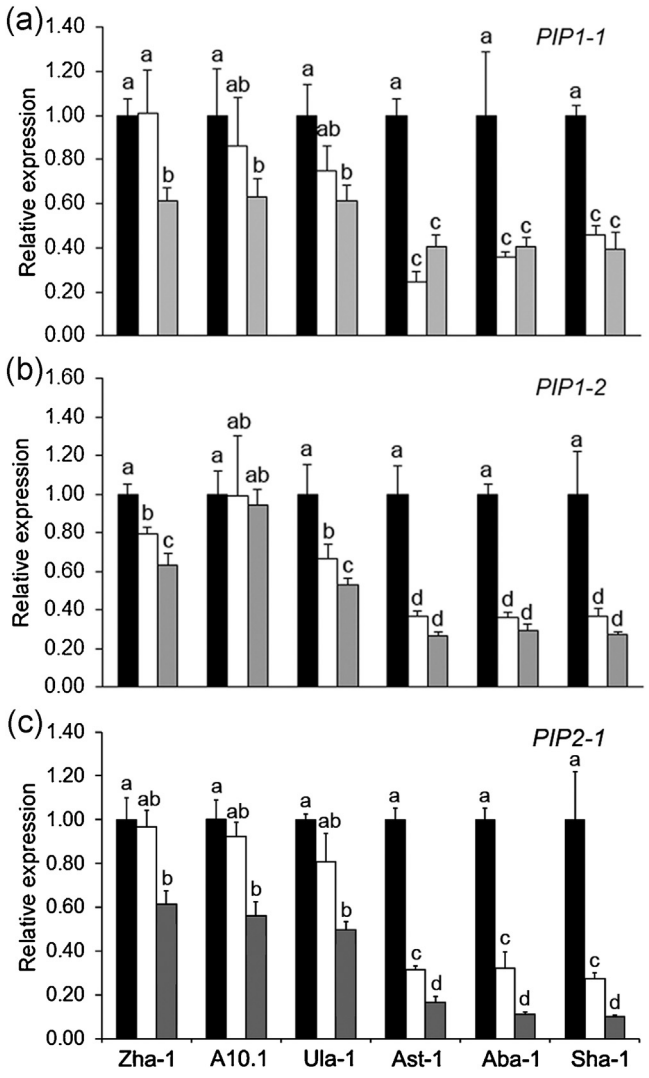

Fig. 4. Assessment of water channel AQP genes from PIP1, PIP2 and TIP subfamilies in *Setaria viridis* accessions under WW, WS and HS conditions. Mean relative expression pattern of (a) *PIP1-1*, (b) *PIP1-2* and (c) *PIP2-1* genes as determined by qRT-PCR, respectively. Black, white and grey bars represent the Mean ± SE (n = 3) of normalized values ($2^{-\Delta\Delta CT}$) from RNA samples of well-water (WW), water stress (WS) and heat stress (HS) treated plants and letters on the bars indicate significant differences at $P \leq 0.05$ level as tested by Tukey-Kramer HSD. See Table S1 for reference and target genes.

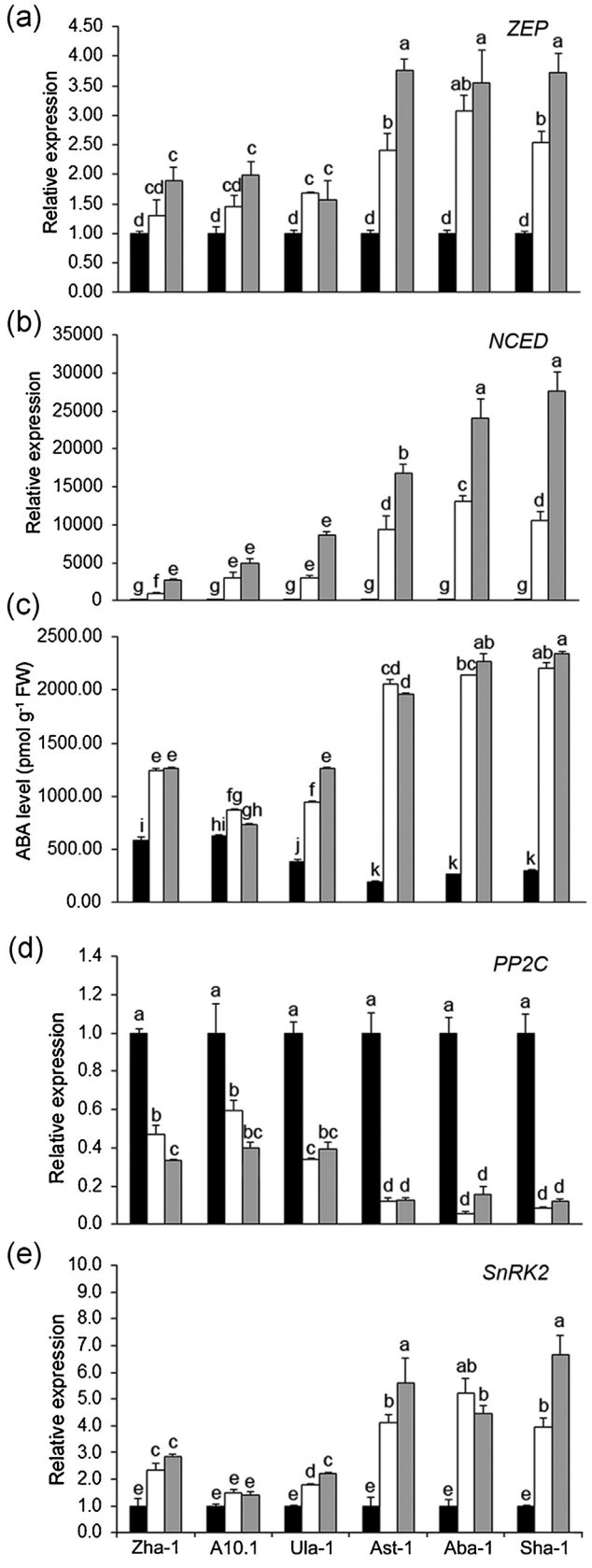

Fig. 5. Quantification of ABA biosynthesis- and signaling-related genes as well as ABA content in *Setaria viridis* accessions subjected to WW, WS and HS conditions. Quantitative measurements of mean relative expression of (a) *ZEP*, (b) *NCED* genes of the ABA biosynthetic pathway as determined by qRT-PCR. Determination of (c) ABA content using ELISA. Expression profile of (e) *PP2C* and (f) *SnRK2* genes of ABA signaling using qRT-PCR. Black, white and grey bars represent the Mean ± SE (n = 3) of normalized values ($2^{-\Delta\Delta CT}$) from RNA samples of well-water (WW), water stress (WS) and heat stress (HS) treated plants and letters on the bars indicate significant differences at $P \leq 0.05$ level as tested by Tukey-Kramer HSD. See Table S1 for reference and target genes. FW = fresh weight.

atively enriched in the cytosol and the chloroplast of mesophyll cells, respectively, while *NADP-malic enzyme* (*NADP-ME*), is mainly abundant in chloroplasts of the bundle sheath cells. Under WS, the expression of *PEPC* did not change significantly in Zha-1, A10.1 and Ula-1 than that of Ast-1, Aba-1 and Sha-1. *PEPC* transcript level decreased significantly compared to the WW condition (Fig. 3c). HS caused significant down regulation of *PEPC* in all the five accessions except in Zha-1 (Fig. 3c). Expression of *NADP-MDH* and *NADP-ME* was significantly down-regulated under WS, while relatively lesser changes were seen under HS (Fig. 3d,e).

To assess the involvement of aquaporins (AQP) in differential regulation of water status under stress, we measured the transcript levels of three *plasma membrane intrinsic proteins* (*PIP1-1*, *PIP1-2* and *PIP2-1*) AQP genes that function as membrane water channels. Under both WS and HS, Zha-1, A10.1 and Ula-1 showed little or no change in the relative expression levels of *PIP1-1*, *PIP1-2 and PIP2-1* whereas a 2-fold down-regulation was observed in Ast-1, Aba-1 and Sha-1 (Fig. 4a–c).

3.4. Divergence of accessions in regulation of ABA biosynthesis and signaling during WS and HS

We examined the effects of WS and HS on the expression level of genes known to be key regulators of abscisic acid (ABA) biosynthesis and signaling pathways in all the *S. viridis* accessions. In the ABA biosynthesis pathway *zeaxanthin epoxidase* (*ZEP*) converts zeaxanthin into antheraxanthin and subsequently to violaxanthin while *9-cis-epoxycarotenoid dioxygenase* (*NCED*) cleaves 9-*cis* xanthophylls to form the precursor of ABA, xanthoxin. The expression of *ZEP* was significantly up-regulated in Ast-1, Aba-1 and Sha-1 under WS and HS, respectively (Fig. 5a). No significant differences in *ZEP* transcript was monitored when Zha-1 and A10.1 in WS as compared to the WW conditions. Ula-1 showed a 1.5-fold significantly higher *ZEP* expression under WS. Under HS up-regulation of *ZEP* transcripts was found to be 2-fold in Zha-1, A10.1 and Ula-1, and 4-fold in Ast-1, Aba-1 and Sha-1 under HS when compared with WW (Fig. 5a). The *NCED* was significantly up-regulated many fold in Ast-1, Aba-1 and Sha-1, and to a lesser extent in Zha-1, A10.1 and Ula-1, under WS and HS (Fig. 5b). Concomitantly, a 7.4- to 10.6-fold increase in ABA level was seen in Ast-1, Aba-1 and Sha-1 (Fig. 5c). Expression of two components of the ABA signaling pathway, *protein phosphatase 2C* (*PP2C*) and *sucrose non-fermenting 1-related protein kinase 2* (*SnRK2*) displayed contrasting patterns. Under stress, a significant decrease in *PP2C* expression was observed in all accessions, while a relatively stronger down-regulation of *PP2C* was seen in Ast-1, Aba-1 and Sha-1 (Fig. 5d). The expression of *SnRK2* was more than 3-fold upregulated in Ast-1, Aba-1 and Sha-1 as compared to 1.5 to 3-fold in Zha-1, A10.1 and Ula-1 (Fig. 5e).

3.5. Stress related molecular and associated biochemical changes due to WS and HS

Although no differences in *catalase* (*CAT*) gene expression were seen under WW (Fig. 6a), WS and HS induced increased *CAT* expression in all accessions and particularly higher in Zha-1 and A10.1 (Fig. 6a). Lower *CAT* expression and catalase activity was seen in Ast-1 (Fig. 6a,b), suggesting a relatively slower ROS-scavenging as compared to Zha-1 and A10.1. The expression of *chlorophyll synthase* (*CS*), a gene that is responsible for chlorophyll biosynthesis in

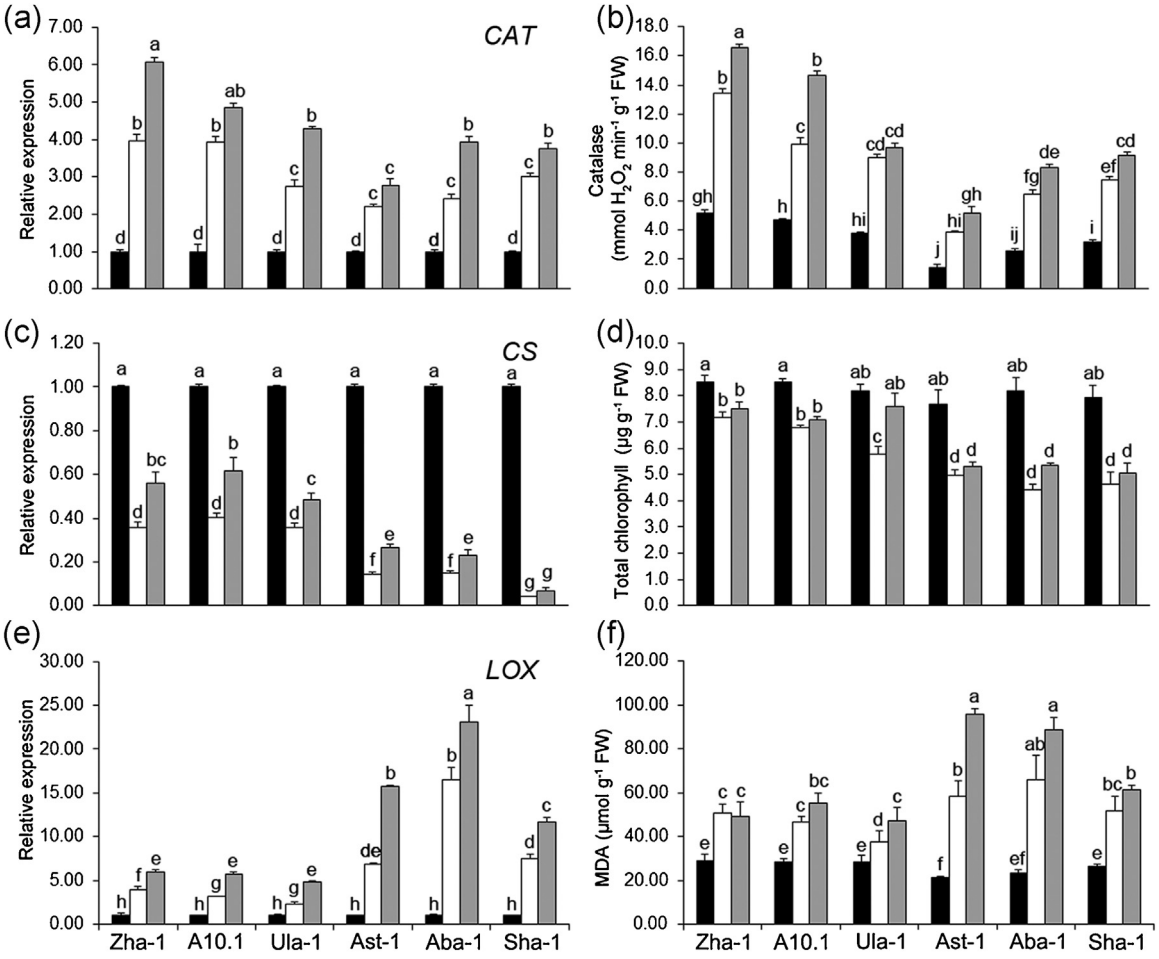

Fig. 6. Monitoring stress related biochemical changes and associated gene expression pattern in *Setaria viridis* accessions under WW, WS and HS treatments. Mean relative expression ($2^{-\Delta\Delta CT}$) of (a) *CAT*, (c) *CS* and (e) *LOX* genes using qRT-PCR. (b) Catalase activity, (d) Total chlorophyll and (f) MDA content at 15 DPT. Data values are the Mean ± SE (n = 3). Black, white and grey bars represent well-water (WW), water stress (WS) and heat stress (HS) treatments and letters on the bars indicate significant differences at $P \leq 0.05$ level as tested by Tukey-Kramer HSD. See Table S1 for reference and target genes. FW = fresh weight.

chloroplasts, was reduced under WS and HS as compared to WW conditions (Fig. 6c). This reduction was higher in Ast-1, Aba-1 and Sha-1. Also, the reduction in chlorophyll contents during WS and HS was less marked than in Ast-1, Aba-1 and Sha-1 (Fig. 6d).

Expression of *linoleate 9S-lipoxygenase* (*LOX*), encoding an enzyme involved in lipid peroxidation was induced by stress in all accessions, but markedly in Ast-1, Aba-1 and Sha-1 (Fig. 6e), with the concomitant increase in MDA content (Fig. 6f). The expression of *pyrroline-5-carboxylate reductase* (*P5CR*), a gene that regulates the last step in proline biosynthesis, and *sucrose-phosphate synthase* (*SPS*) which plays major role in sucrose biosynthesis, were analyzed (Fig. 7). *P5CR* transcripts increased (Fig. 7a), while *SPS* transcripts decreased (Fig. 7c) with stress. The increase in proline contents and the decrease in SPS activity during stress were well correlated with the gene expression trends in all accessions (Fig. 7b,d). A significant decrease in total protein content during stress was seen in accessions Ast-1, Aba-1 and Sha-1 (Fig. 7e). Total sugar contents decreased slightly during WS and HS, but with a marked decrease during WS in accessions Ast-1, Aba-1 and Sha-1 (Fig. 7f).

3.6. Relationships of among physiological, molecular and biochemical properties under WS and HS

We conducted ANOVA of physiological, biochemical and gene expression data to evaluate the significant trait differences among different accessions, stress treatments and the effect of interaction between accessions × stress treatments. Results showed that physiological data were highly significant in all the conditions studied (Table 2). Among biochemical analyses (Tables 3 and 4) soluble sugars (SS) did not show significant differences in all the comparisons tested. Further Pearson Correlation Coefficients (PCC) analysis and hierarchical clustering of physiological, biochemical and gene expression data revealed close relations between Zha-1, A10.1 and Ula-1 (tolerant accessions) and Ast-1, Aba-1 and Sha-1 (sensitive accessions) (horizontal axes of Fig. 8a, b). In the tolerant group, Zha-1 and A10.1 showed the closest clustering under both WS and HS, suggesting that Zha-1 was more closely related to A10.1 than Ula-1 with respect to the stress response(s). In the sensitive group, Ast-1 and Sha-1 showed the closest clustering under WS (Fig. 8a) while Aba-1 and Sha-1 showed the closest clustering under HS (Fig. 8b). When comparing between groups under WS, tolerant Zha-1 and sensitive Ast-1 showed the most distantly related clustering (Fig. 8a), while under HS, tolerant Zha-1 and sensitive Sha-1 showed the most distant related clustering (Fig. 8b). This correlation analyses suggest that Zha-1 > A10.1 > Ula-1 as the most tolerant, while Aba-1 > Sha-1 > Ast-1 as the most sensitive under WS. The ranking for the tolerance response to HS was Zha-1 > A10.1 > Ula-1 > Ast-1 > Aba-1 > Sha-1.

4. Discussion

The progression of global climate change will result in water-deficit and heat stress episodes that cause losses in the agricultural productivity. C4 grasses of the subfamily Panicoideae (comprising

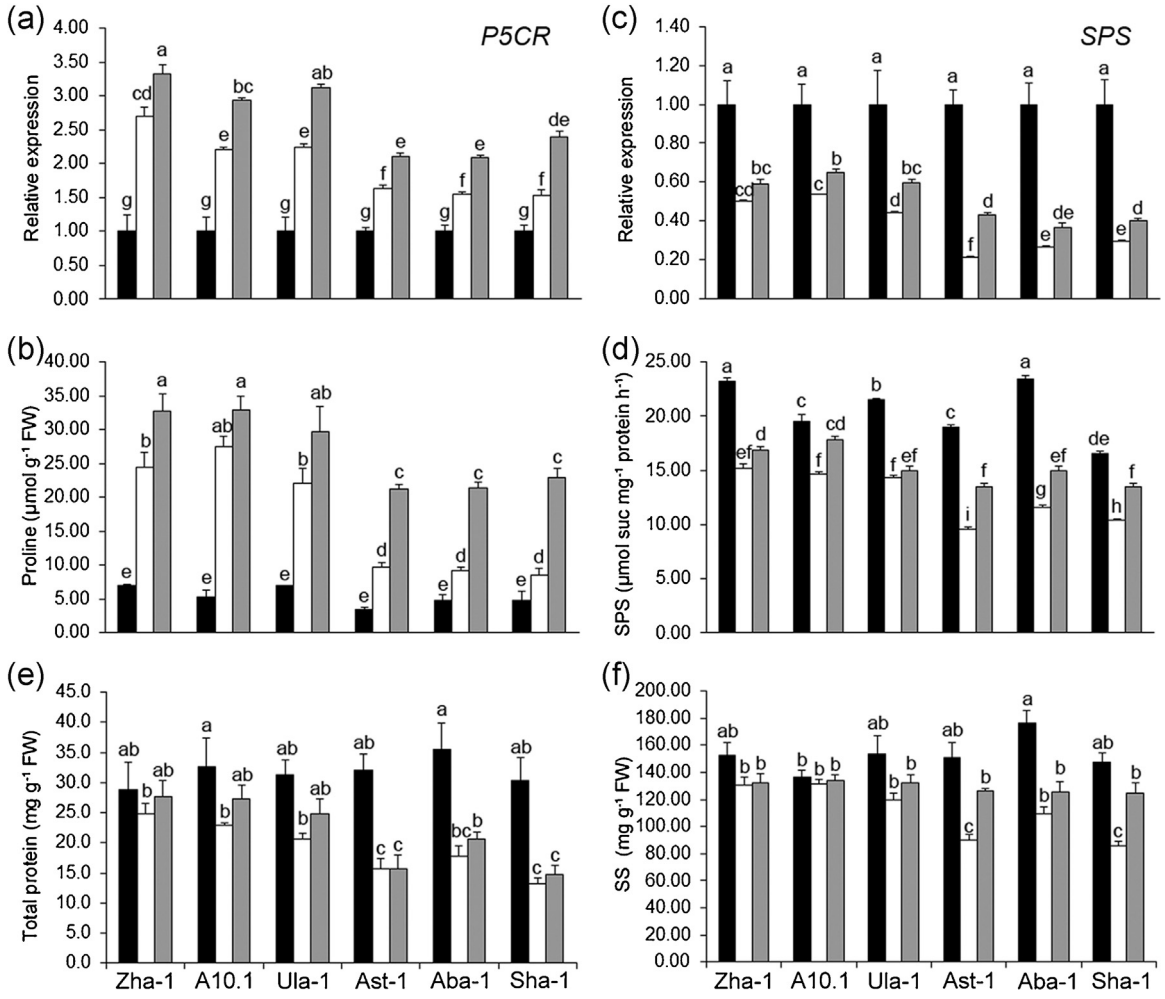

Fig. 7. Stress-related biochemical changes and associated gene expression in *Setaria viridis* accessions subjected to WW, WS and HS treatments. Mean relative expression ($2^{-\Delta\Delta CT}$) of (a) *P5CR* and (c) *SPS* genes using qRT-PCR. (b) Proline and (c) total protein content. (d) SPS activity and (f) soluble sugar (SS) content at 14DPT. Data points represent the Mean ± SE (n = 3). Black, white and grey bars represent well-water (WW), water stress (WS) and heat stress (HS) treatments, respectively, and letters on the bars indicate significant differences at $P \leq 0.05$ level as tested by Tukey-Kramer HSD. See Table S1 for reference and target genes. FW = fresh weight.

Table 2
Results of ANOVA for physiological studies of *Setaria viridis* accessions under three conditions tested (WW, WS and HS).

Parameters	Mean square				
	Stress (S)	Replication (Stress) [Rep(S)]	Accession (A)	S × A	Residual (R)
Leaf water potential (Ψ_{leaf})	17.50**	0.02	1.74**	1.05**	0.03
Photosynthesis (A)	4718.60**	15.10*	581.60**	129.80**	9.35
Transpiration (E)	107.30**	0.36	8.752**	3.18**	0.28
Stomatal conductance (g_s)	0.1676**	0.0006	0.0199**	0.02**	0.00
Dry weight (DW)	94.41**	0.6900	3.276**	2.157**	0.33

Degrees of freedom (*df*) for S = 2, Rep (S) = 24, A = 5, S × A = 10, R = 120.
* Significant at $P < 0.05$.
** Significant at $P < 0.01$.

maize, sorghum, millet and switchgrass, etc.) are well adapted to hot and dry climates [2] and they can make a significant contribution to global food and fuel security [36]. In this respect, *S. viridis* with its C4 photosynthesis and large number of accessions originated world-wide [14–16] provides an exceptional plant model to further extend our understanding on plant water use and heat tolerance. Nevertheless the physiological, molecular and biochemical analyses of *S. viridis* accessions to water-deficit and heat stress tolerance are scanty.

Here, we exposed a number of *S. viridis* accessions, collected from different locations of the world (Table 1), to water-deficit stress and stressful heat stress (high day time temperatures) and demonstrated the physiological plasticity of *S. viridis* accessions to abiotic stress. Our observations in Ast-1, Aba-1 and Sha-1 showed that decreasing Ψ_{leaf} correlated well with the reduced A and g_s under stress (Figs. 1 and 2). The decrease in Ψ_{leaf} (lower than −1.1 MPa) under WS severely reduced photosynthetic rates in Ast-1, Aba-1 and Sha-1 and to a lesser extent in Zha-1, A10.1 and Ula-1 (Fig. 1). A similar response in the reduction of A was reported with decreasing Ψ_{leaf} in C4 grasses under stress [36]. Similarly, A and g_s were more reduced by HS in Ast-1, Aba-1 and Sha-1 than in Zha-1, A10.1 and Ula-1 (Fig. 1). Stress-tolerant switchgrass geno-

Table 3
Results of ANOVA for biochemical studies of *Setaria viridis* accessions under three conditions tested (WW, WS and HS).

Parameters	Mean square				
	Stress (S)	Replication (Stress) [Rep(S)]	Accession (A)	S × A	Residual (R)
ABA	8881015.00*	9793.80	6246727.00*	6395599.00*	2385.00
Catalase	473.60*	1.18	385.80*	73.85*	0.22
Chlorophyll	30.81*	0.17	6.48*	1.07*	0.36
MDA	9080.00*	89.12	474.90*	342.90**	146.60
Proline	2451.00*	21.97	142.40*	38.15	21.68
Protein	847.80*	58.26	123.60**	42.15	47.83
SPS	291.10*	0.56	33.74*	6.80*	0.25
SS	11914.00*	1444.00	1572.00	1266.00	911.20

ABA, abscisic acid; MDA, malondialdehyde; SPS, sucrose-phosphate synthase; SS, soluble sugar. Degrees of freedom (*df*) for S = 2, Rep (S) = 6, A = 5, S × A = 10, R = 30.
* Significant at $P < 0.05$.
** Significant at $P < 0.01$, respectively.

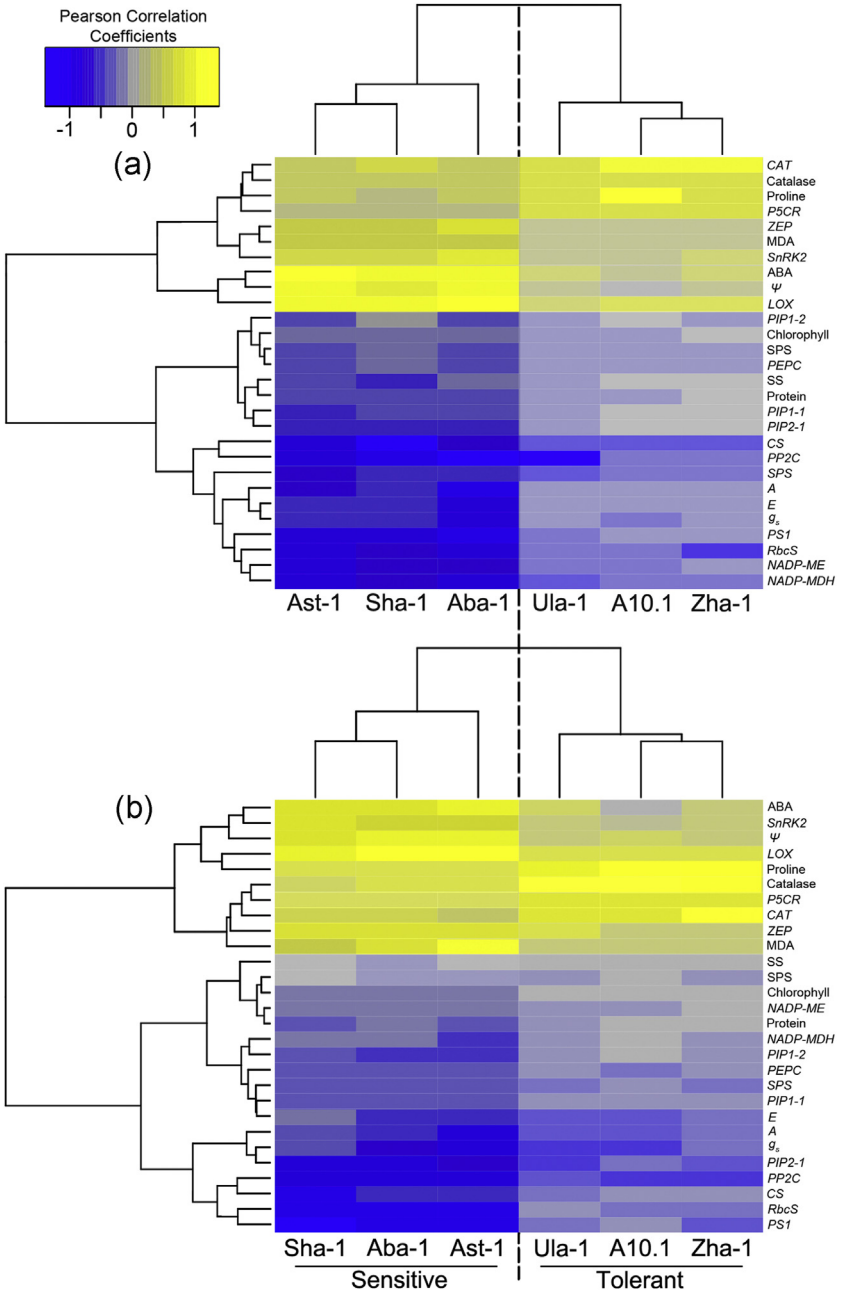

Fig. 8. Visualization of accessions differences in relation to physiological, biochemical properties and gene expression pattern of *Setaria viridis* under WS and HS. Cluster analysis of *S. viridis* accessions with physiological, biochemical and gene expression data under (a) WS and (b) HS as compared with WW. Hierarchical clustering of Log_{10} transformed mean values calculated based on Pearson correlation coefficients and heatmaps showing positive (yellow) and negative (blue) correlation were generated using R statistical software. See Tables 2–4 for physiological, biochemical and gene expression data and gene names.

Table 4
Results of ANOVA for gene expression data of *Setaria viridis* accessions under three conditions tested (WW, WS and HS).

Parameters	Mean square				
	Stress (S)	Replication (Stress) [Rep(S)]	Accession (A)	S × A	Residual (R)
CAT	44.00*	0.07	2.70*	0.95**	0.08
CS	3.10*	0.00	0.12*	0.04**	0.00
LOX	468.00*	0.80	150.00*	43.00**	1.20
NADP-MDH	2.44*	0.10	0.10*	0.04	0.02
NADP-ME	2.10*	0.03	0.10**	0.03	0.03
NCED	1.50*	0.18	0.33*	0.13	0.07
P5CR	1257.00*	2.19	100.00**	27.00**	0.01
PEPC	1.20*	0.04	0.06	0.02	0.03
PIP1-1	1.13*	0.01	0.16**	0.07**	0.03
PIP1-2	1.10*	0.06	0.21**	0.07	0.03
PIP2-1	2.63*	0.01	0.24**	0.10**	0.02
PP2C	4.00*	0.00	0.04**	0.03**	0.00
PS1	3.00*	0.01	0.22**	0.07**	0.02
RbcS	3.10*	0.02	0.17**	0.05	0.03
SnRK2	39.00*	3.10	11.00**	4.00	3.89
SPS	2.40*	0.00	0.02**	0.01**	0.00
ZEP	18.10*	0.70	2.94**	2.70**	0.29

Degrees of freedom (*df*) for S = 2, Rep(S) = 6, A = 5, S × A = 10, R = 30;
* Significant at $P < 0.05$.
** Significant at $P < 0.01$, respectively.

types displayed less decrease in *A* and g_s under drought stress than stress-sensitive genotypes [7], supporting our observations. Therefore, since no significant differences in the total leaf area (which accounts for most of the area for transpiration) were seen among the different accessions (Fig. 2), the lower Ψ_{leaf} including reduced *A*, *E* and g_s in Ast-1, Aba-1 and Sha-1 under stress, suggest the sensitivity of these accessions to WS and HS as compared to Zha-1, A10.1 and Ula-1. The reduced *A* under both WS and HS caused significant reductions of biomass DW in Ast-1 to Sha-1, as compared with Zha-1 to Ula-1, and WHS reduced plant growth to a much greater extent than WS or HS applied separately (see Supplementary Fig. S1 in the online version at DOI: 10.1016/j.plantsci.2016.06.011). These observations suggest that the variation in stress responses among accessions was a consequence of different water use as seen by changes in the Ψ_{leaf} and g_s. This resulted in the changes of *A* which consequently reflected in the differences of biomass DW penalty under WS, HS and WHS.

The analysis of changes in transcriptional activity could advance our understanding on the molecular regulatory mechanisms associated with the response(s) of accessions to WS and HS. However, for the accurate transcript normalization of gene expression data during abiotic stress treatments using qRT-PCR, suitable reference genes are essential [18,19]. We examined a set of reference genes (see Supplementary Table S1 in the online version at DOI: 10.1016/j.plantsci.2016.06.011) and identified a combination of two (*TAU* and *IF4A*) best stable reference genes (see Supplementary Table S2 in the online version at DOI: 10.1016/j.plantsci.2016.06.011) for quantifying changes in transcript levels under abiotic stress conditions in *S. viridis*. Expression level of C4 photosynthesis-related transcripts (*PS1*, *RbcS*, *PEPC*, *NADP-MDH* and *NADP-ME*) was significantly down-regulated in Ast-1, Aba-1 and Sha-1 under the stress conditions when the Ψ_{leaf} was lower than −1.25 MPa (Fig. 2). Supporting these observations, Ghannoum [36] reported 20% to 33% reduced activity of Rubisco, PEPC and NADP-ME enzymes under WS conditions when Ψ_{leaf} was −1.17 MPa and −1.61 MPa in maize and sugarcane, respectively. These results are in agreement with the lower Ψ_{leaf} and poor gas exchange of Ast-1, Aba-1 and Sha-1 under stress. The different response of accessions to Ψ_{leaf} might be a result of osmotic adjustment leading to changes in the root and leaf radial water movement [37]. Radial water movement through xylem is highly regulated by anatomical structure and cellular factors such as AQP membrane water channels [38]. For example, overexpression of *AQP* in various crop plants increased the plants hydraulics and stomatal conductance under abiotic stress leading to tolerance [39,40]. Zha-1, A10.1 and Ula-1 showed a relative high expression of different AQP in the leaf under stress (Fig. 4) which was well correlated with the better Ψ_{leaf}, *A* and g_s of these accessions. On the other hand, Ast-1, Aba-1 and Sha-1 displayed strong decrease in Ψ_{leaf} and less *AQP* expression upon stress (Figs. 1 and 4). These differences in leaf AQP expression, together with the relatively high Ψ_{leaf}, *A*, g_s and proline content in Zha-1, A10.1 and Ula-1 might suggest a better radial flux of water from roots to leaf through an efficient osmotic adjustment.

During WS and HS, the slightly increased *ZEP* and *NCED* transcription and the relatively lower increase in ABA contents (Fig. 5) correlated with a better *E* and g_s (Figs. 1 and 2) and stress tolerance in Zha-1, A10.1 and Ula-1 accessions. In contrast, Ast-1, Aba-1 and Sha-1 accessions showed a marked up-regulation of ABA biosynthesis pathway-associated genes and high ABA contents (Fig. 5). Furthermore, the expression of *PP2C*, a negative regulator of ABA signaling decreased with stress in all accessions, but more markedly in the stress-sensitive accessions (i.e. Ast-1, Aba-1 and Sha-1). On the other hand, the expression of *SnRK2* increased markedly in the sensitive accessions (Fig. 5). Protein kinases of the SnRK2 (SNF-1 Related Protein Kinase 2) were shown to be associated with the accumulation of ABA during stress [41].

The response(s) of plants to abiotic stress is mediated by a number of metabolic/biochemical pathways that determine the ability of distinct plant species to grow under stress [42]. Proline accumulates in many plant species in response to osmotic stress [43], where it acts as a store of carbon and nitrogen and as a scavenger of reactive oxygen species (ROS) [44]. Moreover, the overexpression of *P5CR* resulted in increased stress tolerance in several crops [42]. Abiotic stresses induce the generation of ROS and the enhanced production of ROS-scavenging enzymes has been associated with increased tolerance of plants to water-deficit stress [45]. Catalase, mediating the degradation of H_2O_2, plays important cellular roles protecting cellular damage during stress tolerance [46]. Other stress-induced changes associated with abiotic stresses are chlorophyll degradation, lipid peroxidation, decreased protein and sugar contents, denaturation and reduced carbohydrate metabolism, etc. [45]. Although WS and HS induced changes in the transcription of *CAT*, *CS*, *LOX* and *P5CR* with the consequent changes in catalase, chlorophyll, MDA production, proline and protein contents in all *S. viridis* accessions (Figs. 6 and 7), our results indicated differential transcriptional and metabolic regulations within Zha-1, A10.1 and Ula-1 accessions could lead to stress tolerance. Finally, the lesser effect of stress on Zha-1, A10.1 and Ula-1 on the transcriptional regulation of *SPS* and the higher SPS activity were in good agreement with the better stress tolerance of these accessions.

In conclusion, results of this study shows that the *S. viridis* accessions exhibit plasticity in their physiological, gene expression and biochemical responses to water-deficit and heat stresses. Zha-1, A10.1 and Ula-1 are more tolerant to WS and HS than Ast-1, Aba-1 and Sha-1. A comprehensive comparative transcriptomic and metabolic analysis and its correlation to the distinct phenotypes of the stress tolerant and stress sensitive accessions can be a useful tool for the identification of pathways associated with the responses of Panicoideae C4 grasses to abiotic stress.

Acknowledgments

Authors are thankful to Dr. Ellen Tumimbang, Mrs Elham Abed and Kevin Abernathy for technical support. This work was funded by the United States Agency for International Development (USAID)

to support the Feed the Future Innovation Lab for Climate-Resilient Millet under the Grant No. APS M/OAA/GRO/EGAS-11-002011.

References

[1] J.R. Ehleringer, T.E. Cerling, B.R. Helliker, C4 photosynthesis, atmospheric CO2, and climate, Oecologia 112 (1997) 285–299.
[2] R.F. Sage, X.-G. Zhu, Exploiting the engine of C4 photosynthesis, J. Exp. Bot. 62 (2011) 2989–3000.
[3] T.P. Brutnell, L. Wang, K. Swartwood, A. Goldschmidt, D. Jackson, X.G. Zhu, E. Kellogg, J. Van Eck, *Setaria viridis*: a model for C4 photosynthesis, Plant Cell 22 (2010) 2537–2544.
[4] C.R. John, R.D. Smith-Unna, H. Woodfield, S. Covshoff, J.M. Hibberd, Evolutionary convergence of cell-specific gene expression in independent lineages of C4 grasses, Plant Physiol. 165 (2014) 62–75.
[5] L. Wang, A. Czedik-Eysenberg, R.A. Mertz, Y. Si, T. Tohge, A. Nunes-Nesi, S. Arrivault, L.K. Dedow, D.W. Bryant, W. Zhou, J. Xu, S. Weissmann, A. Studer, P. Li, C. Zhang, T. LaRue, Y. Shao, Z. Ding, Q. Sun, R.V. Patel, R. Turgeon, X. Zhu, N.J. Provart, T.C. Mockler, A.R. Fernie, M. Stitt, P. Liu, T.P. Brutnell, Comparative analyses of C4 and C3 photosynthesis in developing leaves of maize and rice, Nat. Biotechnol. 32 (2014) 1158–1165.
[6] C. Lata, P.P. Sahu, M. Prasad, Comparative transcriptome analysis of differentially expressed genes in foxtail millet (*Setaria italica* L.) during dehydration stress, Biochem. Biophys. Res. Commun. 393 (2010) 720–727.
[7] J.N. Barney, J.J. Mann, G.B. Kyser, E. Blumwald, A. Van Deynze, J.M. DiTomaso, Tolerance of switchgrass to extreme soil moisture stress: ecological implications, Plant Sci. 177 (2009) 724–732.
[8] R.S. Yadav, D. Sehgal, V. Vadez, Using genetic mapping and genomics approaches in understanding and improving drought tolerance in pearl millet, J. Exp. Bot. 62 (2011) 397–408.
[9] P. Saha, E. Blumwald, Spike-dip transformation of *Setaria viridis*, Plant J. 86 (2016) 89–101.
[10] M.V. Mickelbart, P.M. Hasegawa, J. Bailey-Serres, Genetic mechanisms of abiotic stress tolerance that translate to crop yield stability, Nat. Rev. Genet. 16 (2015) 237–251.
[11] A.S. Jump, R. Marchant, J. Peñuelas, Environmental change and the option value of genetic diversity, Trends Plant Sci. 14 (2009) 51–58.
[12] D.J. Layton, E.A. Kellogg, Morphological, phylogenetic, and ecological diversity of the new model species Setaria viridis (Poaceae: Paniceae) and its close relatives, Am. J. Bot. 101 (2014) 539–557.
[13] H.Y. Li, Y.F. Yang, Phenotypic plasticity of life history characteristics: quantitative analysis of delayed reproduction of green foxtail (*Setaria viridis*) in the Songnen Plain of China, J. Integrative Plant Biol. 50 (2008) 641–647.
[14] P. Huang, M. Feldman, S. Schroder, B.A. Bahri, X. Diao, H. Zhi, M. Estep, I. Baxter, K.M. Devos, E.A. Kellogg, Population genetics of *Setaria viridis*, a new model system, Mol. Ecol. 23 (2014) 4912–4925.
[15] G. Jia, S. Shi, C. Wang, Z. Niu, Y. Chai, H. Zhi, X. Diao, Molecular diversity andpopulation structure of Chinese green foxtail [*Setaria viridis* (L.) Beauv.] revealed by microsatellite analysis, J. Exp. Bot. 64 (2013) 3645–3656.
[16] P. Li, T.P. Brutnell, *Setaria viridis* and *Setaria italica*, model genetic systems for the Panicoid grasses, J. Exp. Bot. 62 (2011) 3031–3037.
[17] J.L. Bennetzen, J. Schmutz, H. Wang, R. Percifield, J. Hawkins, A.C. Pontaroli, M. Estep, L. Feng, J.N. Vaughn, J. Grimwood, J. Jenkins, K. Barry, E. Lindquist, U. Hellsten, S. Deshpande, X. Wang, X. Wu, T. Mitros, J. Triplett, X. Yang, C.-Y. Ye, M. Mauro-Herrera, L. Wang, P. Li, M. Sharma, R. Sharma, P.C. Ronald, O. Panaud, E.A. Kellogg, T.P. Brutnell, A.N. Doust, G.A. Tuskan, D. Rokhsar, K.M. Devos, Reference genome sequence of the model plant *Setaria*, Nat. Biotechnol. 30 (2012) 555–561.
[18] P. Saha, E. Blumwald, Assessing reference genes for accurate transcript normalization using quantitative real-time PCR in pearl millet [*Pennisetum glaucum* (L.) R. Br.], PLoS One 9 (2014) e106308.
[19] H.-Y. Kim, P. Saha, M. Farcuh, B. Li, A. Sadka, E. Blumwald, RNA-seq analysis of spatiotemporal gene expression patterns during fruit development revealed reference genes for transcript normalization in plums, Plant Mol. Biol. Rep. (2015) 1–16.
[20] D. Chen, X. Pan, P. Xiao, M.A. Farwell, B. Zhang, Evaluation and identification of reliable reference genes for pharmacogenomics toxicogenomics, and small RNA expression analysis, J. Cell. Physiol. 226 (2011) 2469–2477.
[21] A. Untergasser, H. Nijveen, X. Rao, T. Bisseling, R. Geurts, J.A. Leunissen, Primer3Plus, an enhanced web interface to Primer3, Nucleic Acids Res. 35 (2007) W71–74.
[22] P. Saha, P. Majumder, I. Dutta, T. Ray, S.C. Roy, S. Das, Transgenic rice expressing *Allium sativum* leaf lectin with enhanced resistance against sap-sucking insect pests, Planta 223 (2006) 1329–1343.
[23] P. Saha, T. Ray, Y. Tang, I. Dutta, N.R. Evangelous, M.J. Kieliszewski, Y. Chen, M.C. Cannon, Self-rescue of an EXTENSIN mutant reveals alternative gene expression programs and candidate proteins for new cell wall assembly in Arabidopsis, The Plant J. 75 (2013) 104–116.
[24] M.K. Walker-Simmons, P.A., Rose, L.R., Hogge, S.R. Abrams, Abscisic Acid, in, 2000, pp. 33–47.
[25] P. Saha, I. Dasgupta, S. Das, A novel approach for developing resistance in rice against phloem limited viruses by antagonizing the phloem feeding hemipteran vectors, Plant Mol. Biol. 62 (2006) 735–752.
[26] T. Ray, P. Saha, S.C. Roy, Commercial production of *Cordyline terminalis* (L.) Kunth. from shoot apex meristem and assessment for genetic stability of somaclones by isozyme markers, Sci. Hort. 108 (2006) 289–294.
[27] M.M. Bradford, A rapid and sensitive method for the quantitation of microgram quantities of protein utilizing the principle of protein-dye binding, Anal. Biochem. 72 (1976) 248–254.
[28] S. Elavarthi, B. Martin, Spectrophotometric assays for antioxidant enzymes in plants, Methods Mol. Biol. (Clifton N.J.) 639 (2010) 273–281.
[29] W.P. Inskeep, P.R. Bloom, Extinction coefficients of chlorophyll a and B in *n*,*n*-dimethylformamide and 80% acetone, Plant Physiol. 77 (1985) 483–485.
[30] Z. Zhang, R. Huang, Analysis of malondialdehyde, chlorophyll proline, soluble sugar, and glutathione content in arabidopsis seedling, Bio-protocol 3 (2013) e817.
[31] J.M. Cross, M. von Korff, T. Altmann, L. Bartzetko, R. Sulpice, Y. Gibon, N. Palacios, M. Stitt, Variation of enzyme activities and metabolite levels in 24 arabidopsis accessions growing in carbon-limited conditions, Plant Physiol. 142 (2006) 1574–1588.
[32] M. Reguera, Z. Peleg, Y.M. Abdel-Tawab, E. Tumimbang, C.A. Delatorre, E. Blumwald, Stress-induced CK synthesis increases drought tolerance through the coordinated regulation of carbon and nitrogen assimilation in rice, Plant Physiol. 163 (2013) 1609–1622.
[33] E. van Handel, Direct microdetermination of sucrose, Anal. Biochem. 22 (1968) 280–283.
[34] R Development Core Team, R: A language and environment for statistical computing., in, R Foundation for Statistical Computing, Vienna, Austria, 2010.
[35] C. Ramakers, J.M. Ruijter, R.H. Deprez, A.F. Moorman, Assumption-free analysis of quantitative real-time polymerase chain reaction (PCR) data, Neurosci. Lett. 339 (2003) 62–66.
[36] O. Ghannoum, C4 photosynthesis and water stress, Ann. Bot. 103 (2009) 635–644.
[37] N. Sade, A. Shatil-Cohen, Z. Attia, C. Maurel, Y. Boursiac, G. Kelly, D. Granot, A. Yaaran, S. Lerner, M. Moshelion, The role of plasma membrane aquaporins in regulating the bundle sheath-mesophyll continuum and leaf hydraulics, Plant Physiol. 166 (2014) 1609–1620.
[38] C. Maurel, Y. Boursiac, D.T. Luu, V. Santoni, Z. Shahzad, L. Verdoucq, Aquaporins in Plants, Physiol. Rev. 95 (2015) 1321–1358.
[39] N. Sade, B.J. Vinocur, A. Diber, A. Shatil, G. Ronen, H. Nissan, R. Wallach, H. Karchi, M. Moshelion, Improving plant stress tolerance and yield production: is the tonoplast aquaporin SlTIP2;2 a key to isohydric to anisohydric conversion? New Phytol. 181 (2009) 651–661.
[40] N. Sade, M. Gebretsadik, R. Seligmann, A. Schwartz, R. Wallach, M. Moshelion, The role of tobacco aquaporin1 in improving water use efficiency, hydraulic conductivity, and yield production under salt stress, Plant Physiol. 152 (2010) 245–254.
[41] H. Fujii, P.E. Verslues, J.K. Zhu, Arabidopsis decuple mutant reveals the importance of SnRK2 kinases in osmotic stress responses in vivo, Proc. Natl. Acad. Sci. U. S. A. 108 (2011) 1717–1722.
[42] M. Reguera, Z. Peleg, E. Blumwald, Targeting metabolic pathways for genetic engineering abiotic stress-tolerance in crops, Biochim. Biophys. Acta 1819 (2012) 186–194.
[43] A.J. Delauney, D.P.S. Verma, Proline biosynthesis and osmoregulation in plants, Plant J. 4 (1993) 215–223.
[44] N. Verbruggen, C. Hermans, Proline accumulation in plants: a review, Amino Acids 35 (2008) 753–759.
[45] Z. Peleg, M.P. Apse, E. Blumwald, Chapter 12 – engineering salinity and water-stress tolerance in crop plants: getting closer to the field, in: T. Ismail (Ed.), Advances in Botanical Research, Academic Press, 2011, pp. 405–443.
[46] R. Mittler, E. Blumwald, The roles of ROS and ABA in systemic acquired acclimation, Plant Cell. 27 (2015) 64–70.